

Title	Elucidation of Laser Welding Phenomena and Porosity Formation Mechanism(Physics, Processes, Instruments & Measurements, INTERNATIONAL SYMPOSIUM OF JWRI 30TH ANNIVERSARY)
Author(s)	Katayama, Seiji; Mizutani, Masami
Citation	Transactions of JWRI. 2003, 32(1), p. 67-69
Version Type	VoR
URL	<a href="https://doi.org/10.18910/3685">https://doi.org/10.18910/3685</a>
rights	
Note	

*Osaka University Knowledge Archive : OUKA*

<https://ir.library.osaka-u.ac.jp/>

Osaka University

# Elucidation of Laser Welding Phenomena and Porosity Formation Mechanism<sup>†</sup>

KATAYAMA Seiji\* and MIZUTANI Masami\*\*

## Abstract

Imperfections, especially porosity, are easily formed in deeply penetrating weld fusion zones produced with high power lasers. To investigate the mechanism of porosity formation, welding phenomena, such as laser-induced plume, keyhole behavior, bubble formation and melt flow were observed during CO<sub>2</sub> or YAG laser welding of aluminum alloy and stainless steel plate by using high speed video camera and X-ray transmission real-time imaging systems. It was revealed that the keyhole fluctuated violently in depth and size at slow speeds during continuous wave welding and that the liquid chiefly flowed backwards near the bottom part of a molten pool from the tip of the keyhole. Such keyhole instability and liquid flow induced by evaporation enhanced the generation of bubbles and pores including the shielding gas. On the other hand, at high welding speeds, different main melt flows toward the upper keyhole inlet were induced by metallic vapor jets from the front wall of the keyhole, leading to the reduction in porosity. Consequently, porosity formation mechanism and laser welding phenomena were clarified in terms of keyhole dynamics, vapor jet directions and liquid flows.

**KEY WORDS:** (Laser Welding), (Weldability), (Porosity), (Melt flows), (Keyhole Behavior), (Plume)

## 1. Introduction

Welding with high power CO<sub>2</sub> and YAG lasers has been receiving great attention as a high-quality, high-efficiency and flexible joining technology for the production of deep penetration welds at high speeds. However, a large amount of porosity is easily formed in these deeply penetrating weld metals<sup>1,2)</sup>. Such porosity formation is a serious problem to be solved in laser welding.

In this study, therefore, during high power CW CO<sub>2</sub> or YAG laser welding of aluminum alloy and stainless steel in Ar, He or N<sub>2</sub> gas, a laser-induced plume and surface molten pool motion were observed using a high speed video camera, and keyhole behavior, melt flows and bubble formation inside the molten pool were investigated by utilizing an X-ray transmission real-time observation method.

## 2. Materials, Apparatuses and Experimental Procedure

A 4 kW YAG laser apparatus and a 50 kW CO<sub>2</sub> laser machine were used for welding normally at 3 or 3.5 kW and at 5 to 20 kW in Ar, He or N<sub>2</sub> shielding gas. The YAG laser beam was delivered through an SI fiber of 0.6 mm in diameter and was focused by the focal lenses of

about 200 mm.

Laser induced plasma/plume, keyhole inlet behavior and molten pool motion were observed by high speed video cameras. An arrangement for such observations during CO<sub>2</sub> laser welding is schematically shown in Fig. 1. Welding phenomena inside the molten pool were also observed through X-ray transmission observation

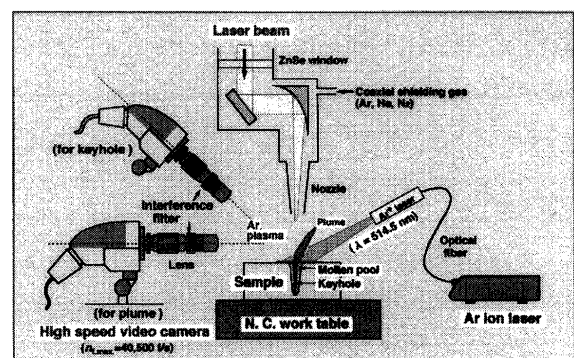


Fig. 1 Schematic arrangement of optical observation system for laser welding phenomena.

<sup>†</sup> Received on January 31, 2003

\* Professor

\*\* Technical Official

## Laser Welding Phenomena and Porosity Formation Mechanism

system. The system together with a YAG laser machine is schematically represented in Fig. 2<sup>1, 2</sup>. This system consists of a microfocussed X-ray tube (160 kV, 1 mA; beam diameters: 10, 20, 50 and 250  $\mu\text{m}$ ), work table, a fluorescent image intensifier, and CCD and high speed video cameras. The materials used are A5083 aluminum alloy with 4.6 %Mg, and Type 304 austenitic stainless steel with 18.3 %Cr and 8.4 %Ni of 6 to 12 mm in plate thickness. Sn or Pt wires and W particles were placed in the holes of the plates for the observation of molten pool geometry and melt flows.

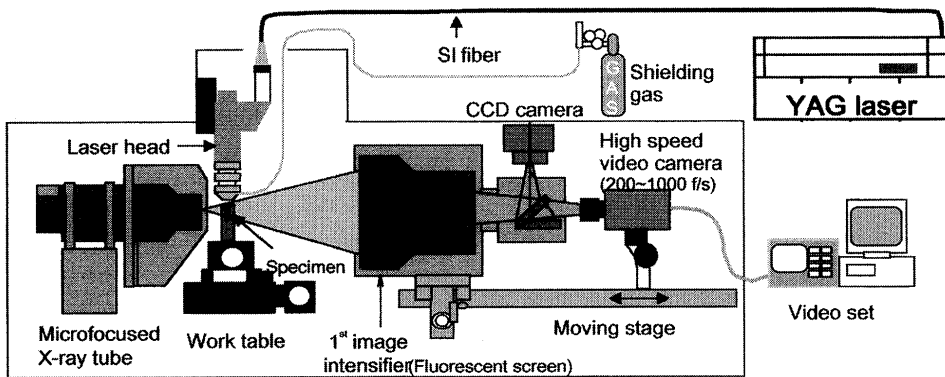


Fig. 2 Schematic arrangement of microfocussed X-ray transmission imaging system for observation of keyhole behavior, bubbles and porosity formation, melt flows in molten pool, and so on.

20 and 10 kW, respectively, at the speed of 10 or 25 mm/s in He shielding gas. In the case of YAG welding of Type 304 in Ar and He inert gas, a keyhole repeatedly expands or shrinks. The tip part of the keyhole swelled frequently up to form a bubble. A wide circulation of bubbles was observed in the molten pool, resulting in the formation of porosity at any penetration location of the weld metal, by entrapment at the side wall of the solidifying front. On the other hand, bubbles and pores were hardly formed during laser welding of Type 304 in  $\text{N}_2$  gas. The N content may be reduced by the reaction with Cr evaporated in the keyhole and plume and by solution into the molten pool.

In the case of  $\text{CO}_2$  laser welding, a keyhole fluctuated intensively, and many bubbles were generated from the tip of the keyhole. All bubbles were trapped near the bottom of the molten pool in Type 304 steel, while they floated up near the solidifying front toward the surface in the molten puddle and some disappeared from the top

### 3. Experimental Results and Discussion

#### 3.1 Keyhole behavior and melt flow during laser welding

A plume, plasma behavior and molten pool surface were observed by high speed cameras. An example of a molten pool during  $\text{CO}_2$  laser welding of Type 304 steel is exhibited in Fig. 3. A laser-induced plume was intensively ejected from a keyhole inlet, and corresponding pool surface motions were recognized.

Keyhole behavior, melt flows, and bubble and porosity formation were observed using an X-ray transmission imaging system. Figure 4 shows examples observed during YAG and  $\text{CO}_2$  laser welding of Type 304 steel and A5083 alloy with Sn wire at the power of 3,

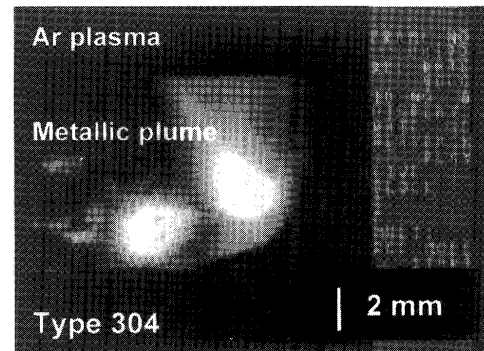
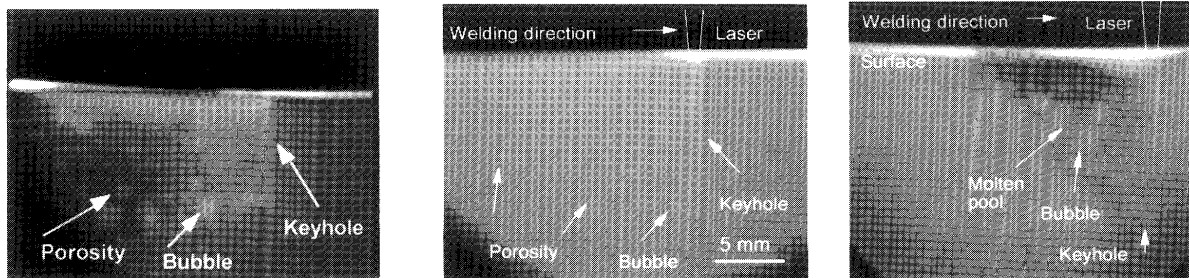


Fig. 3 Molten pool and laser-induced plume and plasma during laser welding of Type 304 steel.



(a) Type 304 at 3 kW

(b) Type 304 at 20 kW

(c) A5083 with Sn at 10 kW

Fig. 4 X-ray transmission observation photos during YAG or  $\text{CO}_2$  laser welding of Type 304 (a), (b) and A5053 with Sn wire (c), showing keyhole behavior, and pore and porosity formation.

surface in A5083 alloy.

The movement of W particles was also observed to confirm melt flows inside the molten pool. The circulation of W particles was seen over a wide range. The rapid speeds measured were 0.4 to 1.2 m/s along the bottom part of the molten pool. It is noted that there is a fast stream across the solidifying front from the bottom part near the keyhole tip to the rear surface of the molten pool. Such W movement or liquid stream is in good agreement with the flow of bubbles, suggesting that the disappearance of bubbles above the surface is not due to the buoyancy effect but due to the melt flow.

### 3.2 Summary of keyhole behavior, liquid flow, and bubble and pore formation during laser welding in inert gas

Keyhole behavior, liquid flow and bubble and porosity formation were observed during welding with CO<sub>2</sub> and YAG lasers under various conditions. It was considered that the keyhole behavior and melt flows were induced by evaporation, depending upon different locations of laser-material interaction and keyhole collapse as well as the content of volatile elements and physical properties such as the vaporization temperature and the surface tension. Such keyhole behavior, melt flows and bubble and porosity formation also depended apparently on the material kind, and welding conditions such as laser power and welding speed. This tendency is schematically summarized as a function of laser, material and welding speed in Fig. 5. Strong and wide liquid flows from the bottom keyhole tip along solidifying front to the rear upper molten pool were recognized especially at slow welding speeds, and many bubbles were generated from the tip part of the keyhole. The bubbles floated along the liquid stream, and became pores after they were captured by the solidifying front. At a higher welding speed, different directions of melt

flows were seen, and the size of bubbles generated was smaller. At extremely high welding speeds, melt flows, different from the case at high speed were prevailing, and no bubbles were formed.

### 4. Conclusions

Major conclusions obtained by high speed video camera and X-ray transmission observation during YAG or CO<sub>2</sub> laser welding of A5083 and Type 304 are the following:

- (1) During cw YAG laser welding in He or Ar gas, a keyhole fluctuated up and down, the liquid flowed down the keyhole and then from the keyhole tip to the rear part of the molten pool. Consequently, many bubbles were generated from the keyhole tip and became pores after they were captured by the solidifying front. In A5083, welded at slow speeds, the majority of bubbles floated up along the liquid flow and disappeared from the top surface of the pool.
- (2) During high power CO<sub>2</sub> laser welding in He shielding gas, the metallic plasma and keyhole were continuously formed, and both of them were unstable because of the local interaction between a laser beam and metallic plasma or the irradiated part, resulting in the formation of many bubbles.
- (3) Porosity was reduced in Type 304 weld beads. This is attributed to low bubble formation probably because of the interaction of Cr and N or N dissolution in the molten pool at the keyhole wall.
- (4) The relationship between keyhole instability, melt flows and bubble generation leading to porosity formation was reasonably well explained over wide ranges of the welding speed.

### Acknowledgements

This research was performed partly under the MITI (Ministry of International Trade and Industry) project of "Development of Advanced Photon Processing and Measurement Technologies". The authors would like to express their deep appreciation to Dr. MATSUNAWA Akira, Prof. Emeritus of Osaka University, and Dr. KIM Jong-Do and Dr. SETO Naoki, Former Graduate Students of Osaka University, for their discussion and assistance to the welding and observation experiments as well as Kawasaki Heavy Industries, Ltd. and AMPI (Advanced Materials Processing Institute, Kinki) for the use of 4 kW YAG laser and 50 kW CO<sub>2</sub> laser apparatus, respectively.

### References

- 1) S. Katayama and A. Matsunawa: Proc. CISFFEL 6, Toulon, (1998), 215-222.
- 2) S. Katayama, N. Seto, M. Mizutani and A. Matsunawa: Proc. of ICALEO 2000, LIA, USA, 89 (2000), Section C-16 ~ 25

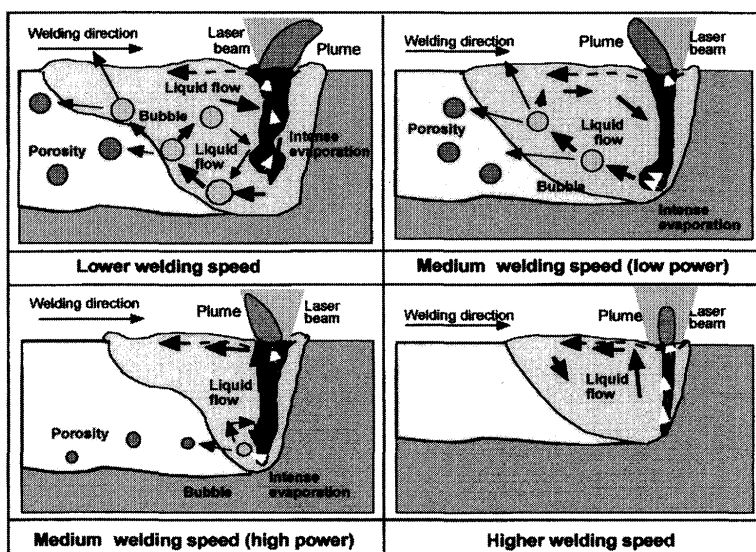


Fig. 5 Schematic summary of keyhole behavior, plume and liquid flows leading to bubbles and porosity formation during cw high power laser welding.